13th World Conference on Earthquake Engineering
Vancouver, B.C., Canada
August 1-6, 2004
Paper No. 2630

ASSESSMENT OF THE SEISMIC BEHAVIOUR OF RC FLAT SLAB BUILDING STRUCTURES

Ema COELHO[1], Paulo CANDEIAS[2], Giorgios ANAMATEROS[2], Raul ZAHARIA[3], Fabio TAUCER[4], Artur V. PINTO[4]

SUMMARY

An experimental program was carried out at the ELSA Laboratory, with the aim of assessing the seismic behaviour of flat-slab structures. The program consisted in pseudo-dynamic tests on a full-scale three-storey RC flat-slab building structure, representative of flat-slab buildings in European seismic regions. The paper presents the experimental results obtained from the two tests, performed using Eurocode 8 compatible accelerograms of increasing intensity, together with the comparison with analytical evaluations. Some considerations are drawn regarding the deficiencies of the behaviour of these structures.

INTRODUCTION

The construction of reinforced concrete buildings with flat slab systems has become widely used in some high seismicity European countries. This type of structures is particularly common in South European countries, such as Italy, Spain and Portugal, both for office and residential buildings. Even though national codes may include rules for the design of these structures, this matter is not covered by the latest draft of Eurocode 8 [1]. The behaviour of this type of structural systems with flat slab frames used as seismic resistant elements show important drawbacks, such as the essentially non-dissipative features of their seismic response. Furthermore, flat slab building structures are significantly more flexible than traditional concrete frame/wall or frame structures, thus becoming more vulnerable to second order P-Δ effects under seismic excitations. Therefore, the characteristics of the seismic behaviour of flat slab buildings suggest that additional measures for guiding the conception and design of these structures in seismic regions are needed, as for instance the possible combination with other seismic resistant structural systems. Together with these rules, additional conditions have to be prescribed, such as the consideration of the low local ductility available or limitations to the form and height of the building.

Considering the aspects above, in the framework of the European Research Network SAFERR and of the European Consortium of Laboratories for Earthquake and Dynamic Experimental Research

---

[1] Principal researcher, National laboratory for Civil Engineering, LNEC, Lisbon, Portugal
[2] Grant holder, National laboratory for Civil Engineering, LNEC, Lisbon, Portugal
[3] Grant holder cat.30, European Commission, Joint Research Centre, IPSC, ELSA, Ispra, Italy
[4] Scientific officer, European Commission, Joint Research Centre, IPSC, ELSA, Ispra, Italy

ECOLEADER, an experimental program was carried out at the ELSA Laboratory of the Joint Research Centre (JRC) in Ispra, Italy, for the assessment of the global behaviour of flat slab structures subjected to severe earthquakes. Two pseudo-dynamic tests, with increasing input intensity, were carried out on a full-scale three storey reinforced concrete flat-slab building structure. The structure, representative of flat-slab buildings in European seismic regions, was tested using artificially generated accelerograms compatible with Eurocode 8 seismic response spectrum. The National Laboratory for Civil Engineering (LNEC) in Lisbon performed the design of the tested specimen, based on the Portuguese design code [2],[3].

DESCRIPTION OF THE STRUCTURE

The tested specimen is a reinforced concrete three storey flat-slab structure, with one bay on each direction. The general layout is show in figure 1. The slab was defined in order to study the failure of the slab-column connections for different situations (interior column, edge column or corner column). For this purpose, two cantilevers were provided, of 1.50m and 1.25m respectively.

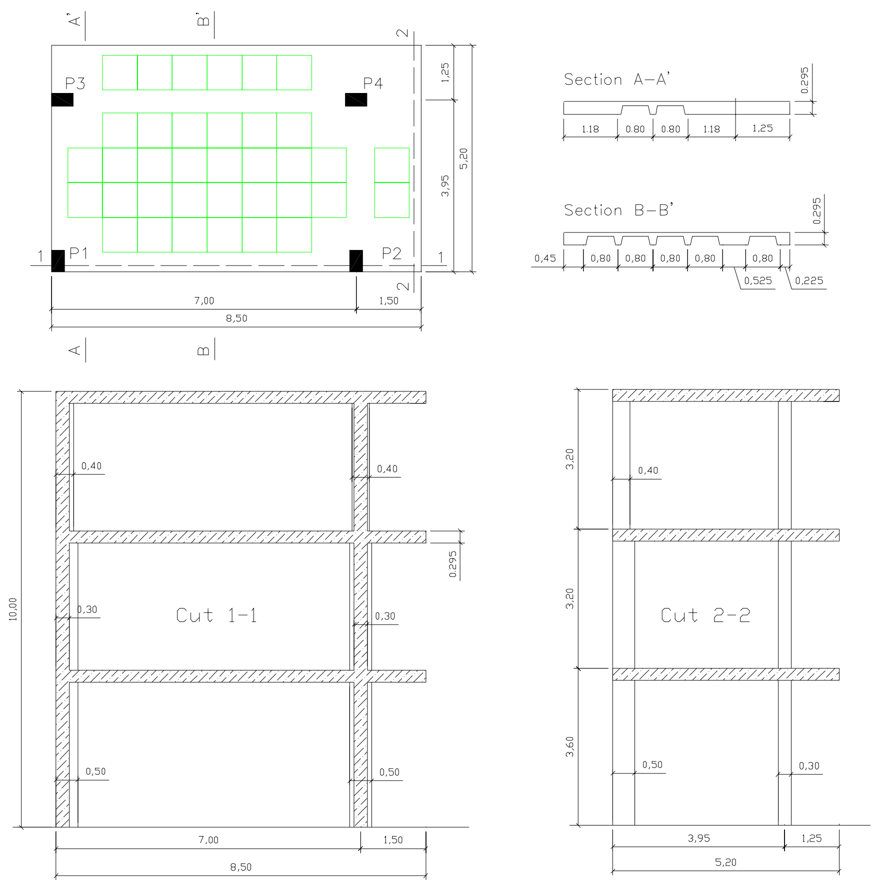

Figure 1. Plan and elevation views of the building

In order to reduce the floor weight, voids of 0.8x0.8m with 0.2m height (waffle slab) were provided in the slab, thus creating wide beams between columns. According to the Portuguese code, in order to account for punching shear, an increased number of stirrups was provided to these beams in the vicinity of slab-column connections. The columns of first and second floor have rectangular cross sections of 0.3x0.5m, while the columns of the third floor have reduced dimensions of 0.3x0.4m. The columns of the South frame (P1 and P2) are differently oriented from the columns of the North frame (P3 and P4).

The materials considered in the design were concrete of class C25/30 and reinforcing steel of class A400. Compressive strength tests on 18 150mm concrete cubes reference specimens, cast during construction lead to an average strength of 37.4Mpa and a corresponding characteristic strength of 34.5Mpa. The reinforcement used in the construction of the specimen was FeB44k Italian steel class, for which the Italian norm specifies a 430Mpa yield strength, 540Mpa for the ultimate strength and an ultimate strain A5 of 14%. Tensile tests on three steel bar specimens from each diameter used in the construction of the model were performed, from which characteristic values of 502Mpa, 619Mpa and 21.9% were obtained for the yield strength, ultimate strength and ultimate strain A5, respectively.

The vertical loads, dead and live loads, in addition to the self-weight of structural elements, were considered to act uniformly along the slabs surface area. The total additional vertical loads for each floor were computed considering the safety factors given by the Portuguese regulations for the earthquake combination and have the following values: 4.2kN/m^2 for office floors (first and second floor) and 3kN/m^2 for terrace (third floor). The self-weight of the slab, considering the voids, is 5.5kN/m^2.

TEST SET-UP

Two pseudo-dynamic tests of the flat-slab building, with increasing input intensity were carried out using the reaction wall experimental facility of the ELSA laboratory. The specimen was tested using artificially generated input motions, of 20 seconds duration, corresponding to a moderate-high European hazard scenario [5]. For the first PSD test, a 475 years return period (475 yrp) was considered, with a corresponding peak ground acceleration of 0.16g. For the second test, the 475 yrp accelerogram was scaled with a factor of 1.73. Thus, the second input motion, with a peak ground acceleration of 0.277g, would correspond to a return period of 2000 years (2000 yrp). The accelerograms are compatible with Eurocode 8 seismic response spectrum. Type 1 response spectrum for soil type D was considered. Figure 2 shows the acceleration time-history and the pseudo-acceleration response spectra for 475 yrp earthquake.

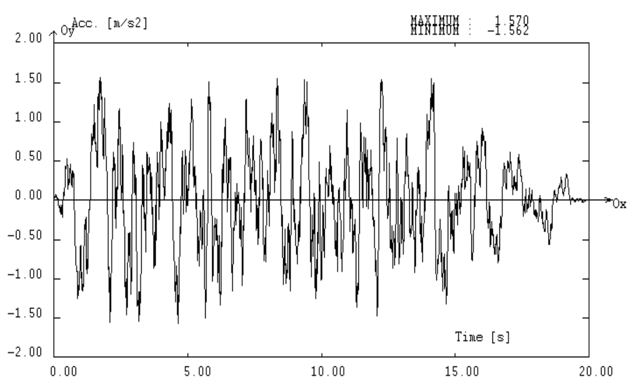

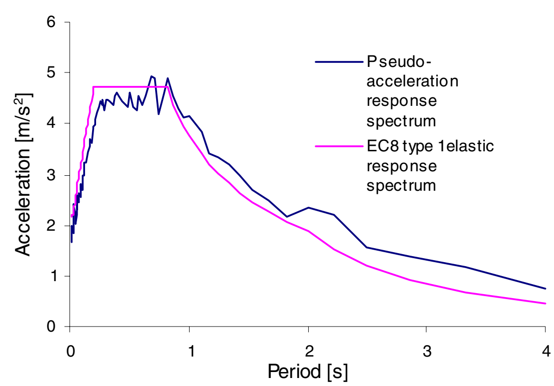

Figure 2. Accelerogram and pseudo-acceleration response spectra for 475 yrp

Figure 3 shows the test set-up. The displacements were applied to the structure by means of six double-acting servo-hydraulic actuators with 500kN maximum load capacity. The structural displacements were measured with respect to an exterior steel unloaded reference frame, mounted on the reaction floor, using Heidenhein optical transducers, which provide a digital output of very high precision. For load application, supplementary concrete beams were provided during construction, on each floor, at mid-span. Additional masses, to simulate permanent loads (other than the self-weight of the slabs) and live loads were placed on each floor by means of large water containers, as shown in figure 3. The weight of the containers was determined considering the presence of the supplementary beam for load application. Thus, the total additional load for each floor was represented by the weight of the containers and the weight of the supplementary beam. The total masses considered in the PSD algorithm for each floor were: 42.9t for first and second floor and 37.5t for the third floor.

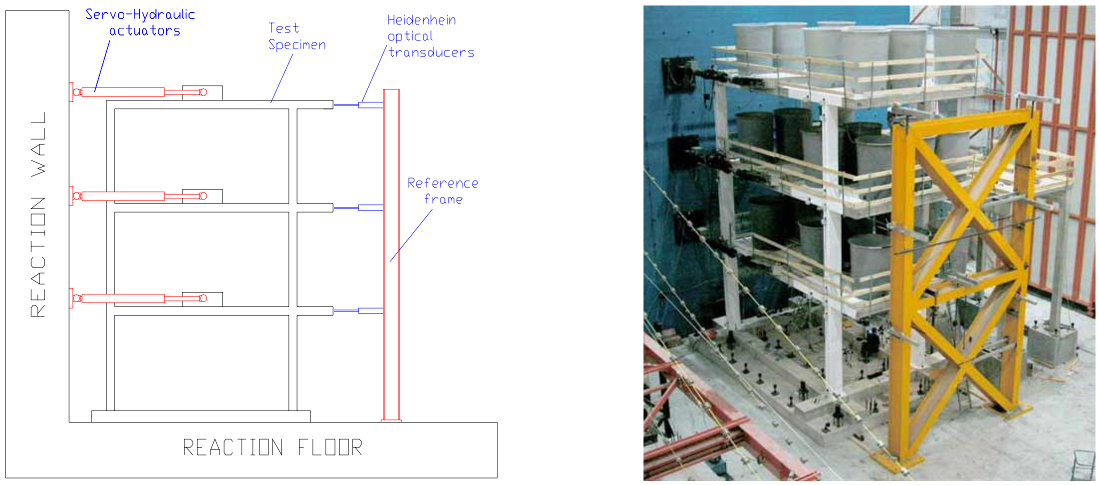

Figure 3. Pseudo-dynamic test – general layout

Rotations were measured by means of 52 digital inclinometers, located around the slab-column connections. Figure 4 shows the location of the inclinometers for the South frame. For the North frame, due to the presence of the cantilever, the inclinometers corresponding to the slab-column joints were positioned on the floor, near the columns. In order to estimate the effective width of the slab, 40 displacement transducers were used on the first floor level around the connections of columns P1 and P3, above and below the slab, as shown in figure 5.

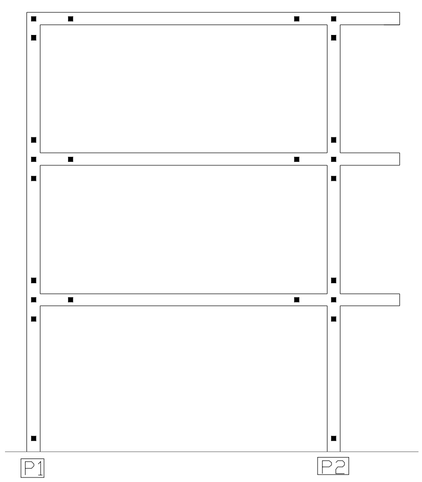

Figure 4. Location of the inclinometers **Figure 5. Displacement transducers**

PRE-TEST NUMERICAL ANALYSIS

In order to predict the behaviour of the flat-slab structure under the considered earthquake input motions, a time – history numerical analysis was performed. Both South and North frames were considered in the numerical model, but only the sections of the primary longitudinal beams were taken into account for analysis. In order to account for the presence of the slab, the nodes corresponding to the beam-column joints of both frames were assumed to have identical displacements, at each level.

The structure was modelled using the fibre/Timoshenko beam element [6] implemented in VisualCast3M computer code. This allows representing the entire reinforced concrete section of the elements, considering both the confined and unconfined parts and also the location of the reinforcement. Concrete behaviour is represented by a parabolic curve up to the peak stress point followed by a straight line in the softening zone [6]. Confinement is taken into account by the modification of the plane concrete curve and including an additional plateau zone. Cyclic behaviour accounts for stiffness degradation and crack closing phenomena. Tensile resistance is also considered. A modified Menegoto-Pinto [7] model with a three-stage monotonic curve (linear, plateau, hardening) represents the steel reinforcement behaviour; Bauschinger effects are taken into account and buckling effects can be simulated.

Under the 475 yrp earthquake, the maximum top displacement obtained from numerical analysis was 169mm, corresponding to a global drift of the structure of 1.71%. The maximum inter-storey drift of 2.04% was obtained at the second storey and it respects, at the limit, the Eurocode 8 requirement of 2%.

The second earthquake input motion was introduced in the numerical analysis after the 475 yrp earthquake, with a 20 seconds zero input acceleration between the two accelerograms, as figure 6 shows. Indeed, in the experimental program, the 2000 yrp earthquake was imposed to the building that had already been damaged. The 20 seconds of zero input acceleration were necessary to stabilise the structure oscillations after the first earthquake. The maximum top displacement obtained from numerical analysis was 249mm, corresponding to a global drift of the structure of 2.52%.

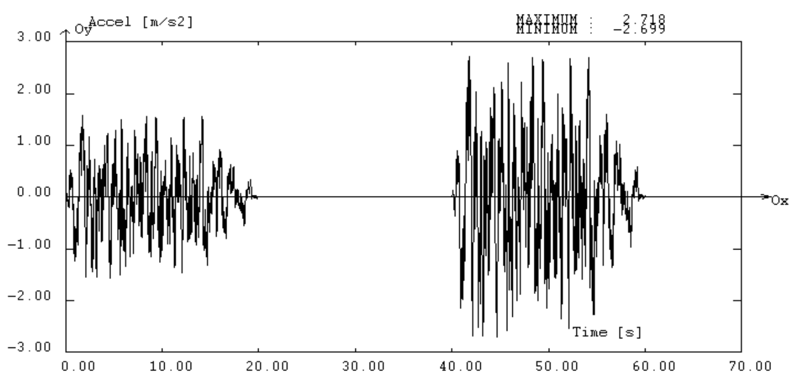

Figure 6. Input motion

The effect of punching shear of slab-column connections was not considered in the numerical analysis. According to recent experimental data and based on some previous researches by Hawkins [8] and Islam [9], Robertson [10] concluded that in flat-slab type structures subjected to lateral loads, the slab-column connections containing shear reinforcement are effective in resisting punching shear failure from 3.5% up to 8% inter-storey drift, depending on the level of the vertical load. The minimal value of 3.5% is granted for a maximum gravity-shear ratio of 0.4. The gravity-shear ratio is defined as the ratio between the initial gravity load transferred from slab to column and the ACI318-99 Building Code [11] direct punching shear capacity of the slab critical section. In case of the tested building, the maximum value for this ratio, for all connections, is lower than 0.4. The structure is also provided with stirrups around the column-slab joints. Consequently, a conservative value of 3.5% inter-storey drift for which the punching shear would not occur, could be considered for the tested specimen. It is expected then, that the failure of the connections to be of the flexural type. The flexural failure is characterised by a smooth decrease of the load-carrying capacity, while the punching failure exhibits a sudden reduction of this capacity (brittle failure) [12].

As for the previous input motion, the numerical simulation of the 2000 yrp earthquake showed that the deformation is concentrated in the second storey, which reaches a maximum drift of 3.04%. This value is lower than the conservative 3.5% limit for punching shear failure. It was expected then that the failure of the connections under the sudden punching shear mode could be avoided and consequently the structure could be safely tested under this input motion. Considering also that the maximum top displacement obtained from the numerical analysis was under the displacement limit of the actuators used in the ELSA laboratory, it was decided that the 2000 yrp earthquake could be used for the second motion input in the PSD test.

EXPERIMENTAL RESULTS

475 yrp earthquake test

Observed damages

Below the slabs, thin flexural cracks developed mainly in the primary beams of South and North frame and in the slab secondary beams, as shown in figure 7, for the second floor. No cracks were identified in the mid-span of the slab. This area corresponds to the supplementary beam for load application, cast together with the slab, thus creating a higher rigidity. At the inferior slab face of the third floor, important cracks were observed around column P3, as shown in figure 8, initiating the slab detachment above the column, due to the insufficient anchorage length of the column reinforcement into the slab.

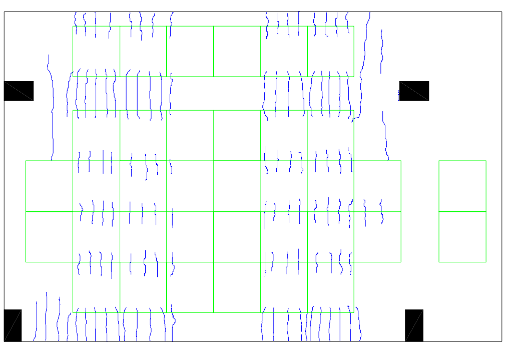

Figure 7. Cracking pattern below floor 2

Figure 8. Slab crack detail around column P3

At first and second floors, above the slab, flexural cracks developed in front of the columns, followed by torsion cracks at approximately 45°, as shown in figure 9 for the second floor. Thicker cracks appeared in the exterior connections of column P1 (corner connection) and P3 (edge connection) due to the torsion failure of the exterior transverse beam. Mainly flexural and some limited torsion cracks appeared around columns P2 and P4, due to the presence of the stronger transverse beam and to concrete confinement. A different cracking pattern, shown in figure 10, was observed at the last floor. Above this slab, the deformation concentrates at the slab-column joints. The cracking pattern around the area corresponding to column P3, indicates that the slab separation initiated above the column. Some thin flexural and shear cracks appeared in columns as well, but only at the base.

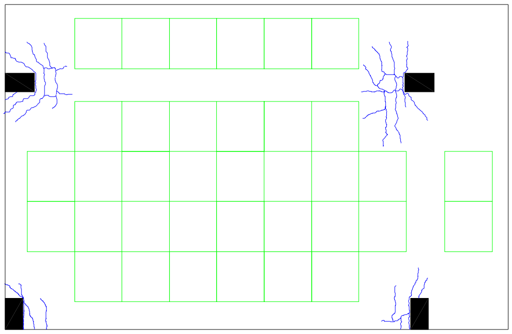

Figure 9. Cracking pattern above floor 2

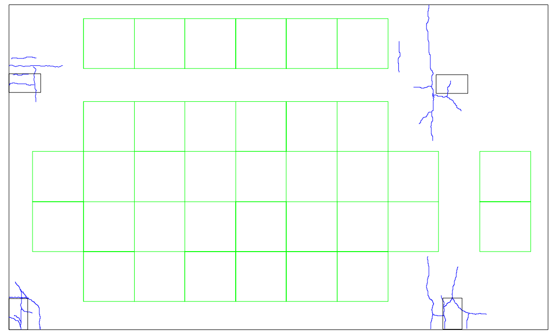

Figure 10. Cracking pattern above floor 3

Results

Figure 11 shows the experimental displacement time-history of the third storey, compared with the corresponding one from numerical analysis. The numerical model proves a good prediction at the level of maximum displacements. The maximum top displacement recorded from experimental data was 162mm, which corresponds to a global drift of 1.64%. A permanent top displacement of 16mm (0.16% global drift) was measured after the test. The displacements are positive when the structure is pulled towards the reaction wall. Figure 12 presents the base-shear versus top-displacement diagram, obtained from the test, also in comparison with the numerical analysis.

Figures 13 and 14 show the comparison between experimental and numerical results in terms of maximum inter-storey drifts and maximum storey shears. As predicted by the numerical analysis, the deformation is concentrated in the second storey. The maximum value of 1.87% of inter-storey drift respects the 2% upper limit recommended by Eurocode 8.

Figure 15 presents the maximum relative rotations obtained at the inclinometer locations, from the experimental data and from numerical analysis, for the North frame. The relative rotations are obtained from the difference of two adjacent inclinometers (the difference between the value of the rotation measured by the inclinometer from slab or column and the reference one from the joint). It is obvious that the deformation is concentrated in the slab-column connections. Similar results were obtained for the South frame. It may be observed that the numerical relative rotations of the slab for the first and second floor, near column P4, are higher than the corresponding ones from the experiment. This is due to the presence of the strong transverse beam between columns P2 and P4, which creates a higher effective width of the longitudinal beam than the width considered in the numerical model.

From visual inspections and confirmed by the results, the deformation in the columns is concentrated at the base. The high value of relative rotation obtained from the test for the top of the P3 column, is due to the separation of the slab over the column, owing to the insufficient anchorage length of the column reinforcement into the slab. Because the reference inclinometers of the North frame at the third floor are placed on the slab in the column axis, the consequence of the phenomenon mentioned above is that the relative rotation of the slab in this case is almost zero. Meanwhile, the reference rotations from the numerical analysis were measured in the intersection points between the slab and the column axis and the numerical model was not able to take into account the insufficient anchorage length.

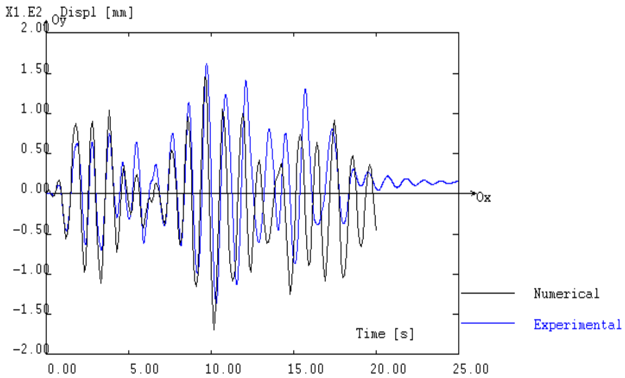

Figure 11. Displacement time history

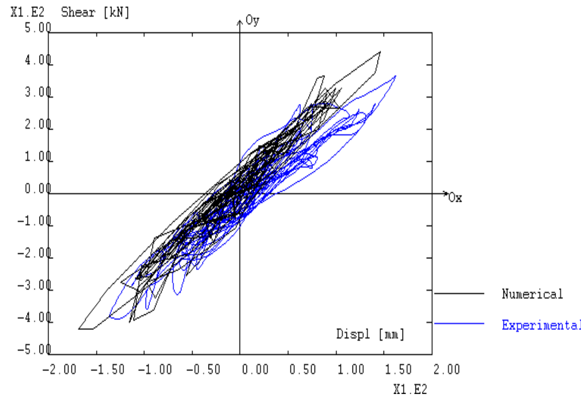

Figure 12. Base-shear versus top-displacement

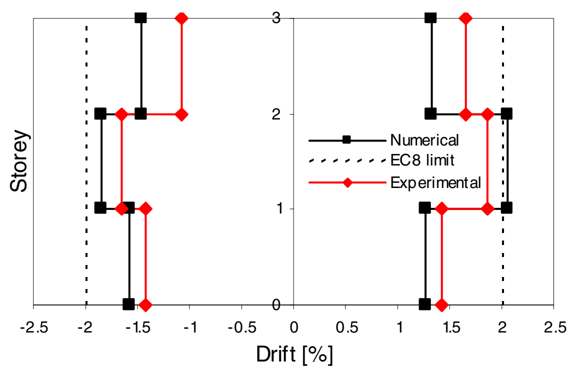

Figure 13. Maximum inter-storey drift profile

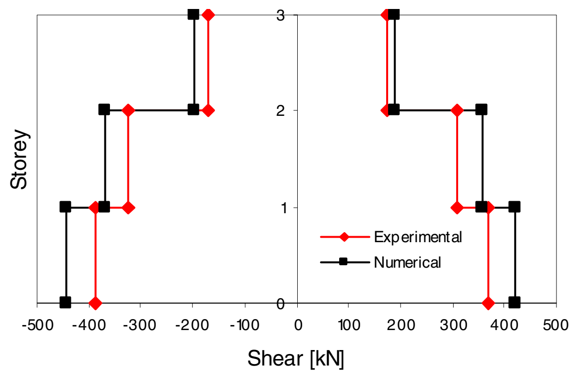

Figure 14. Maximum storey shear profile

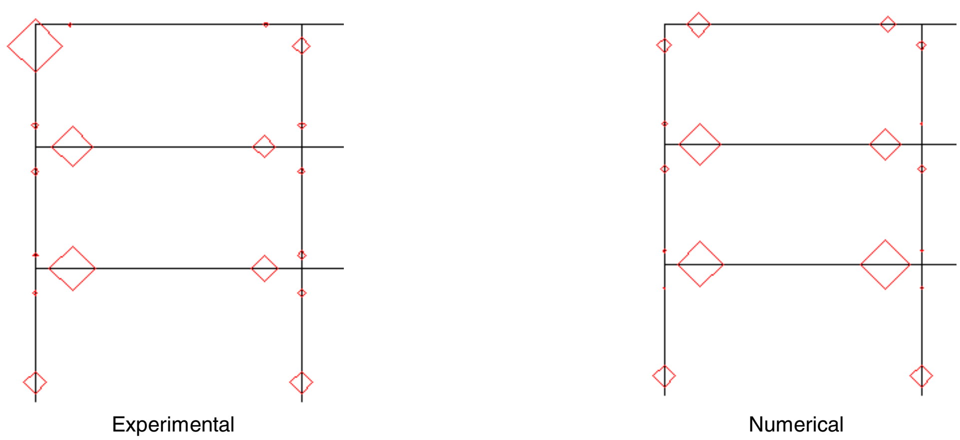

Figure 15. Experimental and numerical maximum relative rotations

2000yrp earthquake test

During the second test, malfunction of one of the actuators lead to the failure of the PSD algorithm and the structure was pulled towards the reaction wall, until the top actuators reached the displacement limit. The structure was heavily damaged and the test had to be stopped at a point corresponding to 2.05 seconds of the accelerogram.

Observed damages

Due to the displacement of the structure towards the reaction wall, important negative moments developed on the exterior slab-column connections of columns P1 and P3. The first test already damaged these connections and torsion cracks developed already in the transverse beam. Consequently, in the second test, the behaviour of the exterior slab-column connections was governed by the torsion failure of the transverse beam. Meanwhile, the displacement towards the reaction wall induced only positive moments in the slab-column connections of columns P2 and P4. Thus, no significant supplementary cracks developed above the slabs.

Below the slabs, due to the positive moment around columns P2 and P4, supplementary cracks of flexural type developed in these regions, new or as extension of the existing ones that resulted from the first test. The cracks that appeared during the second test are marked in red in figure 16, showing the cracking pattern at the second floor below the slab. Important cracks appeared at all floors, on the entire width of the slab, all through the first voids of the East side of the building. Cracks up to 4.0 mm were observed in this area at the first floor; a detail is given in figure 17. Thin cracks also appeared through the entire width of the slab, extending the existing cracks of the secondary beams, thus delimiting the margins of the supplementary beam for load application. Important torsion cracks of the transverse beam developed below the slab around the exterior connections of columns P1 and P3, especially for the edge connection of column P3, as shown in figure 16. Torsion failure of the transverse beam was emphasised for all exterior connections of columns P3 and P1, as shown in figure 18. More pronounced detachment of the slab occurred above column P3 at the third floor, as shown in figure 19.

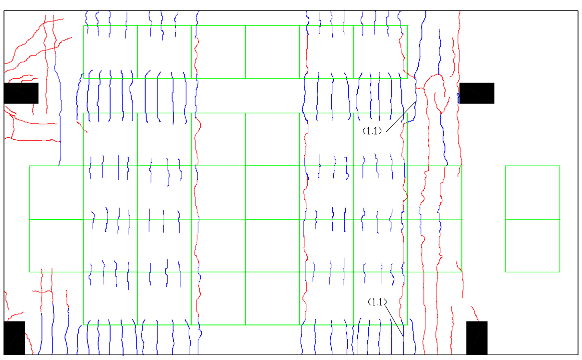

Figure 16. Cracking pattern below floor 2

Figure 17. Slab crack detail

Figure 18. Torsion failure of exterior transverse beam

Figure 19. Detachment of slab above column

Figure 20. Damage at column P3 base

Very thin flexural cracks were observed in the columns above and below the slabs, after the second test. Important damage occurred, however, at the base of columns. Concrete spalling was observed for all column bases and buckling of the reinforcement occurred for column P3, as shown in figure 20.

Results

Figure 23 shows the displacement time-histories for the three storeys. As previously mentioned, the structure was practically pulled towards the reaction wall, up to a maximum top storey displacement of 423mm, corresponding to a global drift of 4.29%. In these conditions, as figure 24 shows, the deformation is concentrated in the first storey, due to the development of plastic hinges at columns base, up to a maximum value of 5.03% drift.

Taking into account the failure of the PSD algorithm, it is not possible to compare the prediction of the numerical time-history analysis for the second input motion with the actual experimental results. However, because it is useful to have a supplementary verification of the finite element model, using the available experimental data, the experimental displacement history was extracted from both tests and then imposed to the numerical model. The comparison between experimental and numerical analysis is then given at the level of base-shear versus top-displacement diagrams (figure 23) maximum storey shear profile (figure 24) and rotations (figure 25). From the storey-shear versus inter-storey drift diagrams it may be observed that there are some differences between the numerical and experimental storey shear at high drift levels, especially for the second and third storey. It must be reminded that the numerical model considered only the beams sections for the analysis, without any slab contribution and no assumptions were made in order to account for the presence of the transverse beam.

Figure 25 presents the absolute rotations measured by the inclinometers during the test, at the maximum global drift of 4.29%, together with the corresponding values obtained from the numerical analysis for the North frame (the arrow shows the displacement direction). The numerical results are generally in good agreement with the experimental ones, excepting for the rotation corresponding to the top of column P3, for the reasons already explained. It may be observed that the rotations measured by inclinometers placed on the slab near exterior column P3 are negligible. Due to the torsion failure of the transverse beam, the slab practically does not rotate in the vicinity of these columns. The same phenomenon was emphasised for the South frame and also for the first test. This demonstrates that the exterior connections could not transfer the bending moments to the column, because of the weak transverse beam, which cracked in torsion at low drift levels. As for the first test, the deformations are concentrated in the slab-column connections and at the base of columns.

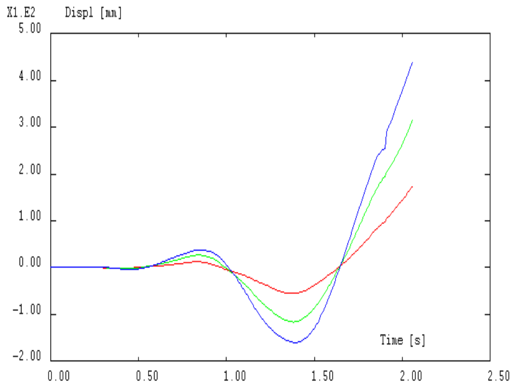

Figure 21. Displacement time-history

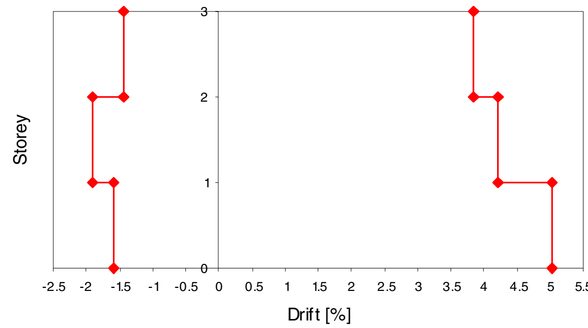

Figure 22. Maximum inter-storey drift profile

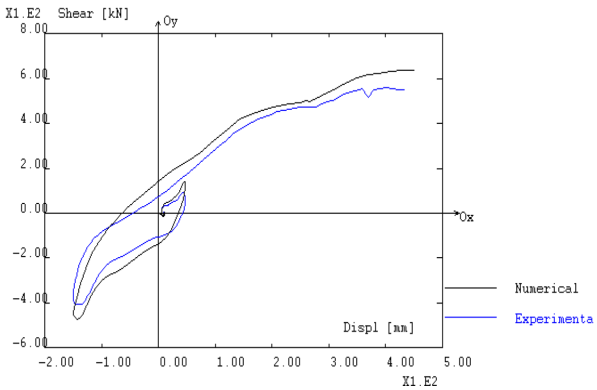

Figure 23. Base-shear versus top-displacement

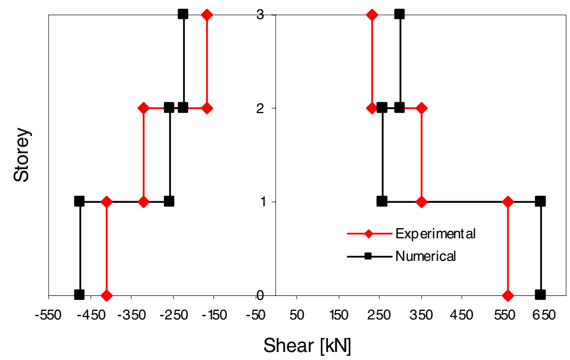

Figure 24. Maximum storey shear profile

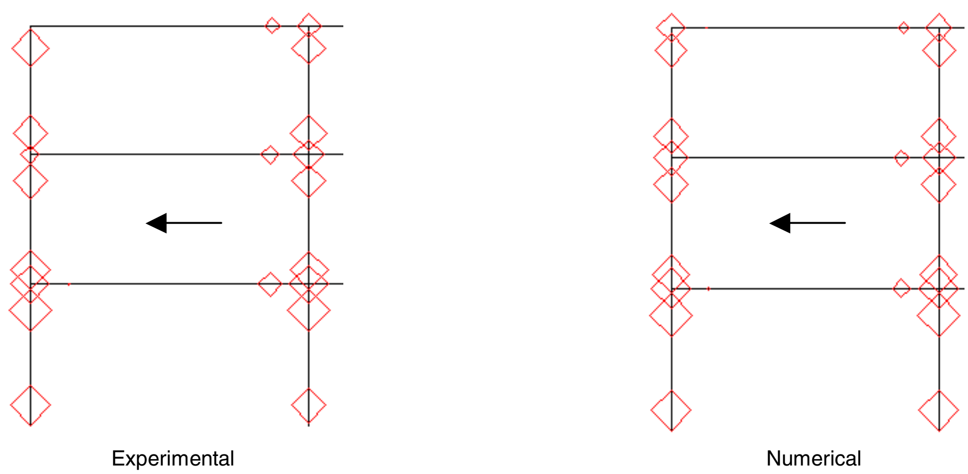

Figure 25. Experimental and numerical absolute rotations at maximum drift

EFFECTIVE SLAB WIDTH

Different studies concerning the effective width of the slab of lateral-loaded slab-column frames have been made, in order to account for the flexural stiffness of the slab. A relatively recent research by

Grossman [13] evaluated several design methodologies based on flat slab-column experimental data and proposed an effective width formula, considering the effects of panel and connection geometry, as well as the lateral drift level:

$$b_{eff} = K_d[0.3L_1 + C_1(L_2/L_1) + 0.5\,(C_2\text{-}C_1)](d/0.9h)K_{FP}$$

in which: K_d is a coefficient function of the drift level, L_1 and L_2 are the lengths of span in direction parallel and perpendicular to lateral load, respectively, C_1 and C_2 are the column dimensions in direction parallel and perpendicular to lateral load, respectively, d is the effective depth of the slab, h is the slab thickness and K_{FP} is a coefficient function of the connection type (1.0 for interior connections, 0.8 for exterior edge connections and 0.6 for exterior corner connections).

In a more recent study by Hwang & Moehle [14], based on experimental data obtained from tests of a 0.4 scale multipanel slab-column frame, the authors proposed a different formula, for exterior connections:

$$b_{eff} =(C_1 + L_1/6)\beta \quad \text{where } \beta = 4C_1/L_1 \geq 1/3$$

This formula is also geometry based, but instead of using a factor accounting for the drift level, a β stiffness reduction factor due to cracking is proposed. Both authors account for the case of exterior/interior connections, but Grossman proposal distinguishes between exterior edge/corner connections.

Flat-slab structures are not considered in Eurocode 8. Eurocode 2 [4], however, offers a methodology for the equivalent frame analysis of this type of buildings. The structure should be divided into frames consisting of strips of slabs contained between centre lines of adjacent panels. The stiffness of these equivalent beams, computed based on the gross cross section of the slab, must be reduced to half in case of horizontal loading, to reflect the increased flexibility of flat-slab structures.

The effective widths of the slab for the exterior connections of the flat-slab building tested at the ELSA laboratory were computed from experimental data at different drift levels. Figure 26 gives the values of the slab deformation, computed from the displacements given by the transducers above and below the first floor slab (figure 5), function of the distance from column P1 to P3 (distance zero is corresponding to column P1 axis). These values are corresponding to the maximum drift of first floor, of 5.03%, obtained from the second test. The peaks of deformation correspond to the displacement transducers placed on the beams axis. Effective width of the slab, for each connection, is computed as the ratio between the area of the corresponding deformation-distance diagram (until centre-line of slab, between column P1 and P3) and the maximum value of the deformation measured in the longitudinal beam.

Figure 27 gives the equivalent effective slab widths, calculated at mid-height of the slab, for negative drifts between 0.38% and 1.59% and positive drifts between 0.38% and 5.03%. The effective slab width b_{eff} is represented as a function of the b_{eff}/b_w ratio, in which b_w represents the actual width of the beam. It may be observed that for the corner connection of column P1, at maximum drift, the effective width of the slab is practically equal to the beam width. For this connection, all the longitudinal reinforcement of the beam passes through the column core. Meanwhile, for the edge connection of column P3, the effective width of the slab is less than the width of the beam. In this case, part of the beam reinforcement passes outside the column core and consequently the ability of the beam to be fully effective in transferring moment relays on the torsion capacity of the transverse beam, which demonstrated a poor behaviour during the first test.

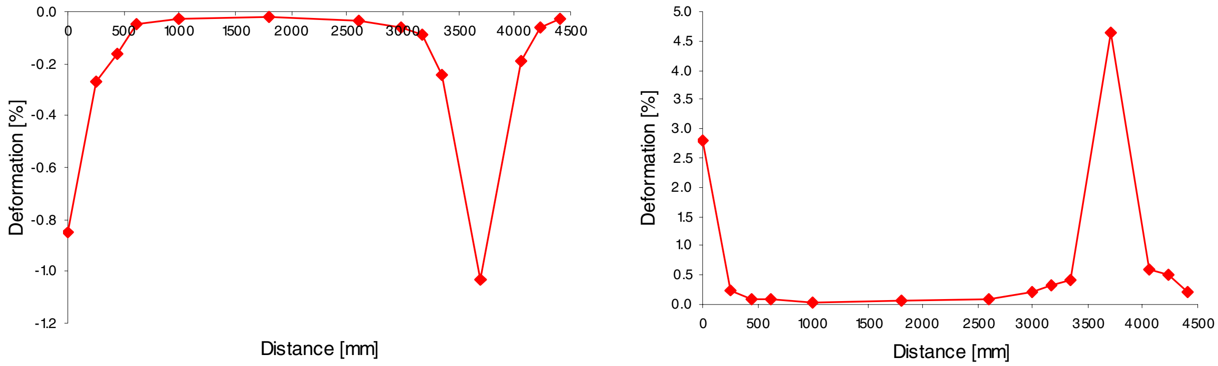

Figure 26. Slab deformation at 5.03% drift (below and above slab)

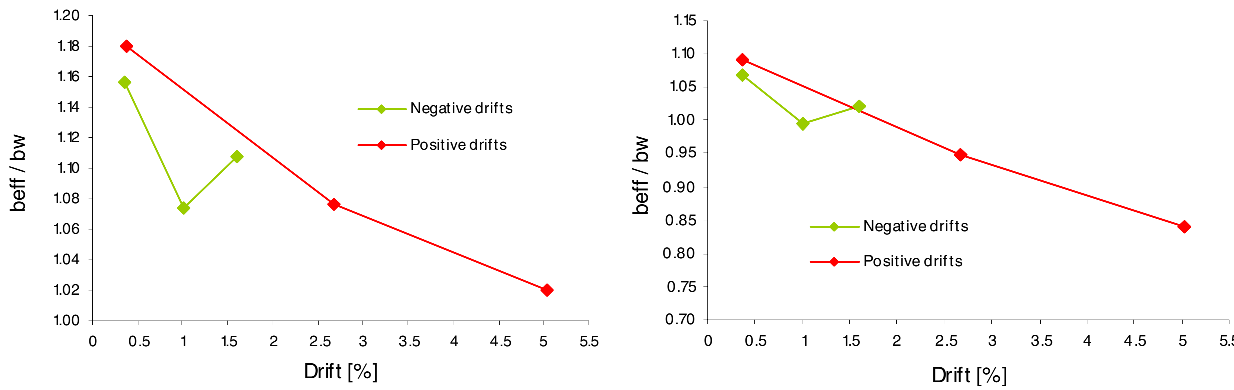

Corner connection (column P1) Edge connection (column P3)

Figure 27. Slab effective width

Tables 1 and 2 present the comparison between the experimental effective widths of the slab in comparison with the results from the above mentioned design methodologies. Both minimum and maximum values of effective widths obtained from the experiment are presented, corresponding to the maximum/ minimum drifts considered for the computation. The two values presented for Eurocode 2 [4] methodology, are computed for the slab section near the columns, considering the reduced number of slab voids and for the current slab section at mid-span, considering all the slab voids. The Grossman [13] value for the effective width was computed for a maximum lateral drift of 1%, as considered by the author. In case of edge connection of column P3, which represents a typical wide beam-column connection, a supplementary design methodology by LaFave & Wight [15] was considered. Based on experimental results, these authors present a simple expression for computing the effective tension slab width in exterior connections with wide beams. The effect of the lateral drift level is included, up to a value of 4%. The formula is (using the same notations as in the previous equations):

$$b_{eff} = 0.5\,(b_w + C_2) + 2C_1$$

in which b_w is the width of the wide beam.

Table 1. Effective widths of slab for column P1 connection [cm]

Experiment Min	Experiment Max	EC2	Grossman	Hwang & Moehle
49.8	57.5	54.4/ 81.6	55.5	48

Table 2. Effective widths of slab for column P3 connection [cm]

Experiment Min	Experiment Max	EC2	Grossman	Hwang & Moehle	LaFave & Wight
50.4	65.5	85.9/ 115	74	54.1	145

The values from Table 1 and 2 show that the best fit with the experimental results are given by the Hwang & Moehle proposal. The value of 54.1cm for the effective slab width of the P3 column connection, can be considered acceptable in comparison with the minimum value of 50.3cm obtained from the experiment, at 5.03% drift. The value of 54.1cm for effective width corresponds in the experiment to a drift around 4%.

Excepting for Hwang & Moehle formula, no other methodology offers results in the safe side for both connections. It must be underlined, however, that a wide range of design detailing exists for slab-column connections in flat-slab structures and that the effective width of the slab, in case of exterior connections, is directly related to the torsion behaviour of the transverse beam.

CONCLUSIONS

Two pseudo-dynamic tests on a full scale flat-slab model of a three storey RC structure, representative of existing flat-slab structures in European seismic areas, were carried out at the ELSA laboratory.

Important flexural and torsion cracks appeared around the exterior slab-column connections. Considerable damage of these connections, due to the torsion failure of the transversal beam was observed at all floors. Mainly flexural and, to a lesser extent, torsion cracks, developed in the other connections, due to the presence of the stronger transverse beam and to the confinement of the concrete. Failure of the slab-column joints, by separation of the slab above the level of the third floor, owing to the insufficient anchorage length of the column reinforcement into the slab, was also observed. The test results also confirm the findings of recent studies concerning the small slab participation under lateral loads.

It is underlined that these structures exhibit significant higher flexibility compared to traditional frame structures becoming more sensitive to second order effects. In order to limit deformation demands under earthquake excitations, combination with other stiffer structural systems as shear-walls is advisable.

AKNOWLEDGEMENTS

Part of the research was carried out at the Joint Research Centre, Ispra, Italy. The tests were financed by the European Commission (DG Research) under FP5–Access to Research Infrastructures [Contract HPR–CT-1999-00059 (ECOLEADER-JRC)]. Raul ZAHARIA is a JRC Cat. 30 grant-holder (Contract No. 20135-2002-11 P1B30 ISP IT).

REFERENCES

1. CEN prEN 1998-1-1:200X Eurocode 8: “Design of structures for earthquake resistance – Part 1: General rules, seismic actions and rules for buildings” Doc CEN/TC250/SC8/N335, Comitée Européen de Normalisation, Brussels, Draft January 2003
2. REBAP - Regulamento de Estruturas de Betão Armado e Pré-esforçado: 1983
3. RSA - Regulamento de Segurança e Acções para Estruturas de Edifícios e Pontes: 1983
4. CEN Eurocode 2: “Design of concrete structures – Part 1: General rules and rules for buildings” ENV 1992-1-1:1991-CEN/TC250/SC2 Comitée Européen de Normalisation, Brussels: 1999
5. Campos-Costa A., Pinto A. V. “European seismic hazard scenarios – an approach to the definition of input motions for testing and reliability assessment of civil engineering structures” JRC Special Publication, No. X.99XX, JRC, Ispra, Italy
6. Guedes J., Pegon P., Pinto A. V. **“**A Fibre/ Timoshenko Beam Element in CASTEM 2000” Special Publication Nr. I.94.31, EC, Joint Research Centre, Institute for Safety Technology, 1994
7. Menegoto M., Pinto P. “Method of analysis for cyclically loaded reinforced concrete plane frames including changes in geometry and nonelastic behaviour of elements under combined normal force and bending” IABSE Symposium on resistance and Ultimate deformability of Structures, Final Report, Lisbon, 1973
8. Hawkins W. H., Mitchell D., Hanna S. N. “Effects of shear reinforcement on the reversed cyclic loading behaviour of flat plate structures” Canadian Journal of Civil Engineering 1975; 2: 572-582
9. Islam S., Park R. “Tests on slab-column connections with shear and unbalanced flexure”. ASCE Journal of Structural Division 1976; 102 (ST3): 549-568
10. Robertson I. N., Kawai T., Lee J., Enomoto B. “Cyclic testing of slab-column connections with shear reinforcement”. ACI Structural Journal 2002; 99(5): 605-613
11. ACI Committee 318 “Building code requirements for structural concrete (ACI 319-99) and Commentary (318R-99)”. American Concrete Institute, Farmington Hills, Michigan, 1999
12. Menétrey P. “Relationships between flexural and punching failure”. ACI Structural Journal 1998; 95 (4): 412-419
13. Grossman J. S. “Verification of proposed design methodologies for effective width of slabs in slab-column frames”. ACI Structural Journal 1997; 94 (2): 181-196
14. Hwang S. J., Moehle J. P. “Models for laterally loaded slab-column frames”. ACI Structural Journal 2000; 97(2): 345-352
15. LaFave J. M., Wight J. K. “Reinforced concrete exterior wide beam-column-slab connections subjected to lateral earthquake loading”. ACI Structural Journal 1999, 96(4): 577-585